The effect of Fe doping on structural and magnetic properties of nanocrystallite $Co_2Cr_{1-x}Fe_xAl$ Heusler alloys prepared by mechanical alloying

M. Hakimi†, P. Kameli, and H. Salamati

Department of Physics, Isfahan University of Technology, Isfahan 84156-83111, *Iran*

(Received 20 April 2012; revised manuscript received 8 July 2012)

Mechanical alloying has been used to produce nanocrystallite $Co_2Cr_{1-x}Fe_xAl$ ($x = 0$, 0.4, 0.6, 1) Heusler alloys. The formation of the $L2_1$ phase of $Co_2Cr_{1-x}Fe_xAl$ by the mechanical alloying method was investigated. The effect of Fe doping on the structural and magnetic properties of the samples was also studied. The results were compared with the Slater Pauling prediction. A comparison between these samples and those prepared by the arc-melting method in the literature was made. An increase of the coercivity H_c with the increasing Fe doping level was observed. This phenomenon was explained by the increases of lattice strain and magnetic anisotropy with the increasing Fe content.

Keywords: magnetic property, X-ray diffraction, nanocrystallite, mechanical property

PACS: 75.30.Cr **DOI:** 10.1088/1674-1056/21/11/117502

1. Introduction

Recently, electronic devices using the spin of electrons, i.e. spintronics, have attracted much scientific attention. Half-metallic ferromagnets (HMFs) have also attracted considerable attention due to their potential use as highly spin-polarized current sources in spintronics.[1−4] HMFs exhibit semiconducting behaviour in one spin band at the Fermi level (E_F), and in the other spin band, they are strongly metallic, which result in a 100% spin polarization at E_F. To date, four types of HMFs have been proposed by theoretical calculations, including oxide compounds,[1] perovskites,[2] zinc-blende compounds,[3] and Heusler alloys.[4] Moreover the Heusler alloys with the general formula X_2YZ, where X and Y are transition metals and Z is an s or p group element, are of interest from both fundamental and practical points of view.

Surprisingly, the properties of many Heusler compounds can be predicted by simply counting the number of valence electrons.[5] For example, non-magnetic Heusler compounds with approximately 27 valence electrons are superconductors.[6] In addition more than 250 compounds are semiconductors and are considered to be novel materials for energy application.[6] Their band gaps can easily be tuned from 0 eV to $\sim$ 4 eV by changing their chemical compositions. Thus, they have attracted considerable attention for the potential use in solar cell and thermoelectric applications.[6] From recent electronic band structure calculations, a new class of Heusler compounds have been discovered: multifunctional topological insulators, i.e. a new state of matter, in which the spin-polarized edge and the surface states are topologically protected against impurity scattering.[7] The introduction of multifunctionality, i.e. the combination of two or more functions, such as superconductivity and topological edge states in one material, is achievable in ternary compounds.[7] The large class of magnetic X_2YZ compounds show all kinds of magnetic behaviours and multifunctional magnetic properties, such as magneto-optical,[8] magnetocaloric,[9,10] and magneto-structural phenomena.[11]

Theoretically, the saturation magnetization M_s of the Heusler compounds obeys the simple Slater Pauling model.[6] According to that model, M_s is directly related to the number of valence electrons and can be calculated as[6]

$$M_s = N_v - 24, \tag{1}$$

where N_v denotes the number of valence electrons per formula unit. In many cases, the experimental result

†Corresponding author. E-mail: m_hakimi@ph.iut.ac.ir

© 2012 Chinese Physical Society and IOP Publishing Ltd

deviates from the theoretical value. For example, Inomata *et al.*[12] have reported a value of 1.1 μ_B for the magnetic moment of $L2_1$-Co_2CrAl thin films, while the value obtained by the model is 3 μ_B. In another work, a value of 4.6 μ_B was obtained for the M_s of Co_2FeAl, which is also lower than the corresponding Slater Pauling value.[13] Furthermore, different values of M_s have been obtained for samples prepared by different methods.[12−14] The magnetic properties of the Co-based Heusler alloys are strongly correlated to the lattice ordering. Since the preparation method of the Heusler alloys plays a significant role in their magnetic behaviours, the influence of the method on the magnetic properties is important.

Polycrystalline samples of Co_2MAl (M = Cr, Fe, Mn) have been commonly synthesized by arc-melting in a noble gas atmosphere. For example, Sabine *et al.*[15] investigated the structural properties of $Co_2Cr_{1-x}Fe_xAl$ particles fabricated by arc-melting. The mechanical alloying (MA) route is a convenient method for preparing nanostructured materials. This method is suitable for the production of novel, high-performance, and low-cost materials, such as ferrites, manganites, intermetallics, and Heusler alloys.[16−21] In comparison with the arc-melting, the MA method is more cost-effective and is able to process powders on larger scales. Recently, Hatchard *et al.*[18] have explored the MA technique for processing Ni–Mn–Ga Heusler alloys. Vinesh *et al.*[19] investigated the effect of ball milling on the magnetic properties of Fe_2MnAl Heusler alloys. Mikami *et al.*[21] have used the MA for the preparation of Fe_2VAl Heusler alloys. We have successfully used this method to synthesis Co_2CrAl and Co_2FeAl compounds in our previous studies.[22,23] The presence of Cr in the Heusler compounds results in a deviation of M_s from the Slater Pauling value, which is related to the antiferromagnetic coupling of the Cr atoms.[28] The magnetic coupling constant is affected by the distance between the Cr atoms. This distance also depends on the Cr concentration and the lattice order of the compound. Investigating the effect of Fe substitution for Cr on the magnetic properties can lead to a better understanding of the effect of milling on the lattice order. Here we synthesize the $Co_2Cr_{1-x}Fe_xAl$ compounds by the MA to study the effects of Fe substitution at the Cr site on the structural and the magnetic properties of these compounds.

2. Experiment

High purity Co, Fe, Cr, and Al powders of 99.9% nominal purity were used as the raw materials. The Al powder was in flake form with an approximate particle size of 10 μm, the Fe powder was composed of spherical particles of similar size. The agglomerated Co and Cr powders used were particles of submicron size. The powders with stoichiometric composition $Co_2Cr_{1-x}Fe_xAl$ (x = 0, 0.4, 0.6, 1) were mechanically alloyed in a planetary ball mill (Fritsch pulverisette P6) in an argon atmosphere. The experiments were carried out at room temperature using 20 mm diameter hardened steel balls and 500 ml stainless steel containers. The ball-to-powder weight ratio and the rotational speed were 10:1 and 300 rpm, respectively. To prevent overheating the containers, the ball-milling was carried out by alternating between 60 minutes of milling and 10 minutes of rest. Following predetermined time intervals (0 h, 1 h, 2 h, 5 h, 10 h, and 15 h), samples of about 500 mg were taken for X-ray diffraction (XRD) and other tests. XRD measurements were performed using a Philips X'PERT MPD diffractometer (Cu $K\alpha$ radiation, λ = 0.154 nm). The crystallite size and the lattice distortion were calculated using the Williamson–Hall equation. Rietveld refinements were performed in order to determine the lattice parameters and the space groups of the samples. The microstructure of the samples was analyzed by scanning electron microscope (SEM), (Philips XL 30). The AC susceptibility measurements were performed using a Lake Shore AC susceptometer (Model 7000). The magnetic properties were characterized by vibrating sample magnetometery (VSM).

3. Results and discussion

3.1. Structural results

Figure 1 shows the XRD patterns measured at room temperature for the unmilled mixture of raw materials for all four compounds. As expected, the XRD pattern of the unmilled mixture contains only the individual reflections of Co, Cr, Fe, and Al phases. Noticeably, Co appears in both fcc and hcp phases in all the samples. The intensity ratios of the individual reflections are almost in accordance with the stoichiometric mixture compositions. The lattice structures of

Cr and Fe are approximately the same, and the Bragg peaks of these two materials are located close to each other. Here there is no discernible difference in the XRD patterns of the samples.

Nevertheless, the XRD patterns of the samples show small changes at two angles, 82° and 99°. As can be seen in the insets of Fig. 1, the changes appear as the annihilation and creation of two peaks. This phenomenon is due to the fact that the atomic radius of Cr is smaller than that of Fe.

To study the formation mechanism of $Co_2Cr_{1-x}Fe_xAl$ compounds, the XRD patterns of the milled powders have been taken and presented in Fig. 2. The insets of Fig. 2 show the evolutions of the diffraction lines of Co and Al.

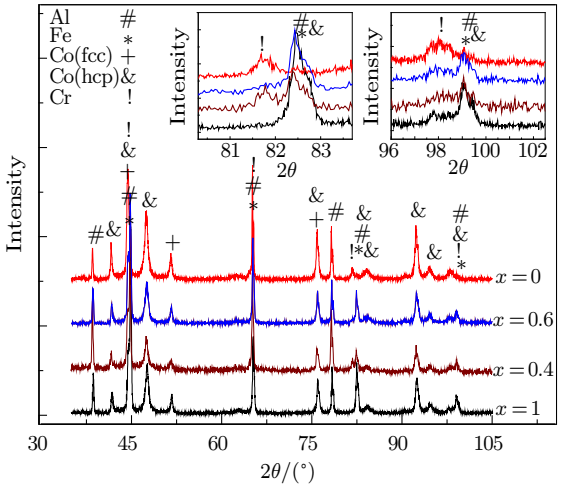


Fig. 1. (colour online) The XRD patterns at room temperature for the unmilled mixture of raw materials of $Co_2Cr_{1-x}Fe_xAl$ compounds. Insets show the changes of the two diffraction lines located at $2\theta = 82°$ and 99°.

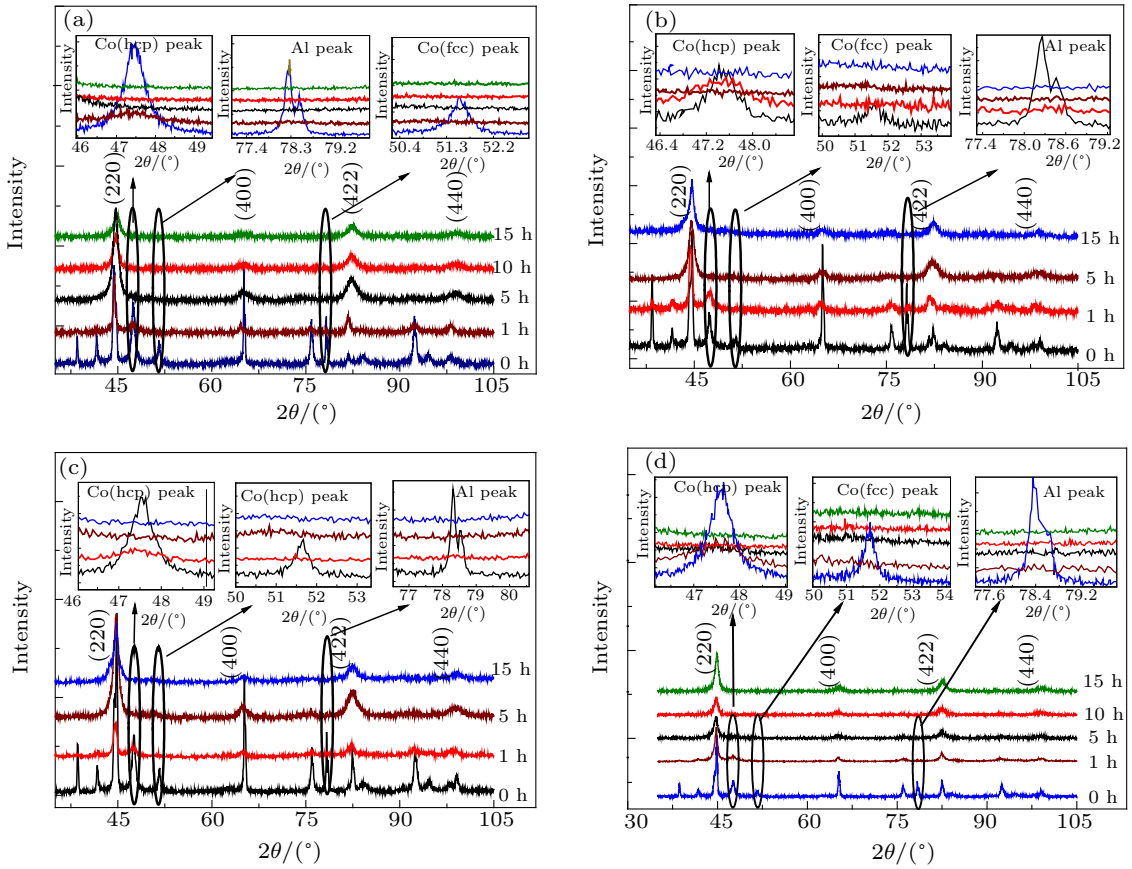


Fig. 2. (colour online) The XRD patterns of the $Co_2Cr_{1-x}Fe_xAl$ samples after different milling time ((a) $x = 0$, (b) $x = 0.4$, (c) $x = 0.6$, (d) $x = 1$). Insets show the dependences of the diffraction lines of Co and Al on the milling time.

As can be seen, by increasing the MA time, the intensities of the diffraction peaks of Al and Co (fcc-structure) quickly decrease, and after one hour of milling, these peaks almost disappear. The analysis of the X-ray data confirms the existence of the CoAl phase in the samples obtained after one hour of MA. The Co (hcp) features are different. Further milling leads to a reduction in intensity and the subsequent disappearance of the Bragg peaks of this material. With the increased Fe content, the reduction in peak

intensity over time is not as rapid. This phenomenon can be related to the catalytic effects of Cr.[24]

It seems that the XRD patterns of the 15 h ball-milled powders are similar to those of $L2_1$-$Co_2Cr_{1-x}Fe_xAl$ Heusler phases. The Miller indices shown in Fig. 2 are related to the $Fm3m$ space group. The Rietveld refinement confirms that the compounds with a milling time of more than 10 h are single phase and have the $L2_1$ structure with the $Fm3m$ space group.

The Rietveld refinement patterns of the 15 h milled samples are presented in Fig. 3. Experimental data (red symbols), theoretical data (black line), the difference between them (blue line), and the Bragg positions (green line) are shown in the figure. The lattice parameters obtained by the Rietveld fittings are shown in Table 1. These lattice parameters are in good agreement with the previous work.[25] The χ^2 parameter as a criterion for matching the calculation and the measurement is also reported in Table 1. The crystallite size and the lattice strain of the L_{21}-$Co_2Cr_{1-x}Fe_xAl$ Heusler phases are estimated using the Williamso–Hall equation. The Williamso–Hall equation is expressed in the following form:[26]

$$B\cos(\theta) = 2(\varepsilon)\sin(\theta) + k\lambda/D, \qquad (2)$$

where B is the full width at half maximum (FWHM) of the XRD peak, k is the Scherrer constant, D is the particle size, λ is the wavelength of the X-rays, ε is the lattice strain, and θ is the Bragg angle.

The results of the crystallite size and the lattice strain are summarized in Table 1. It is evident that the internal lattice strain increases with the increasing Fe content. This phenomenon could be related to the difference of Fe and Cr atomic radii. Since Fe, Cr, and Al are coordinated octahedrally in the L_{21} Heusler phase,[6] the different atomic radii of Cr and Fe, compared to that of Al, influence the lattice strain.

Figure 4 shows the typical SEM images for 0 h, 1 h, and 15 h milled samples (x = 0, 0.4, 1). In the unmilled samples, the elemental materials are distinguishable from one another. The 1 h milled samples show relatively broad distributios of agglomerates composed of the strongly welded particles of different morphologies with particle sizes of about 50 μm.

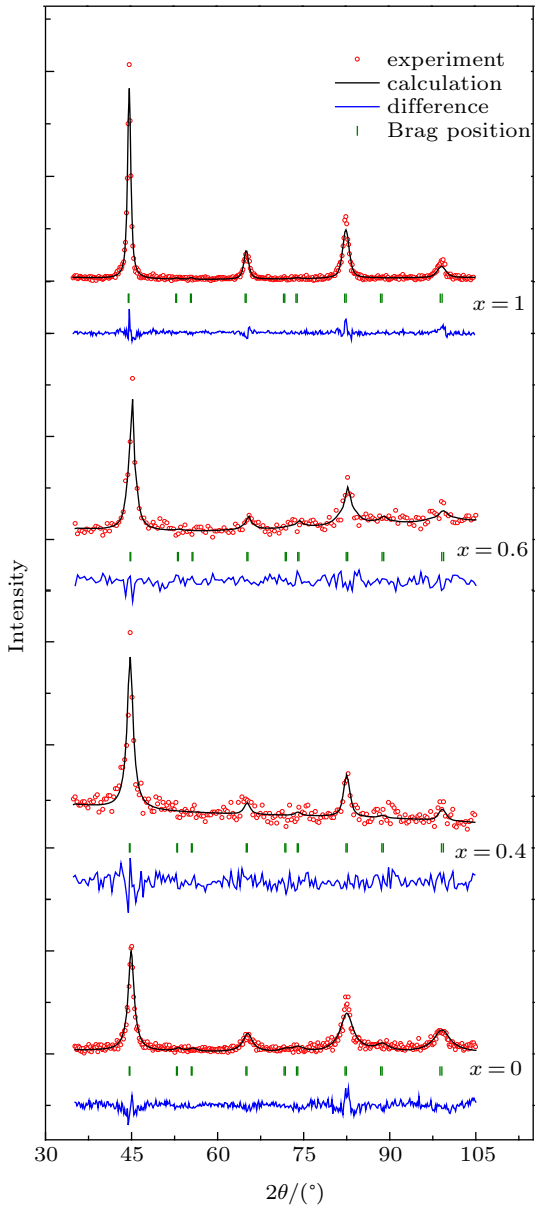


Fig. 3. (colour online) The Rietveld refinement patterns for 15 h milled samples.

Table 1. Selected structural and magnetic parameters of the samples extracted from our measured data. The last column gives the results from the literature.

Sample	Structural parameters					Magnetic parameters			
	Structure	χ^2	Lattice parameter/nm	Crystallite size/nm	Lattice strain	H_c/Oe	M_r/μ_B	M_s/μ_B	M_s/μ_B
Co_2FeAl	$L2_1$	1.39	0.573	19	0.0063	71	0.416	4.4	4.6[13]
$Co_2Fe_{0.6}Cr_{0.4}Al$	$L2_1$	1.38	0.573	10	0.0044	62	0.289	2.7	3.8[13]
$Co_2Fe_{0.4}Cr_{0.6}Al$	$L2_1$	1.18	0.572	12	0.0022	46	0.142	1.9	2.9,[13] 2.2[14]
Co_2CrAl	$L2_1$	1.61	0.574	14	0.0014	36	0.064	1.1	1.1,[12] 0.7[13]

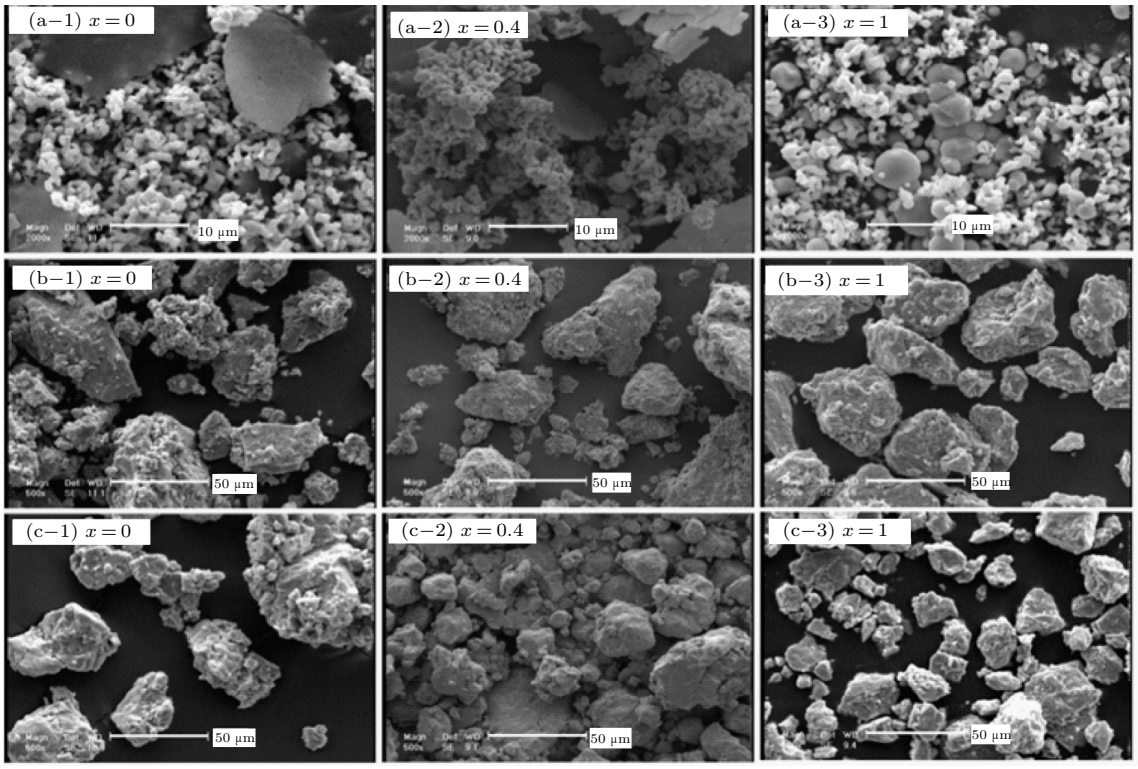


Fig. 4. Typical SEM images for (a) 0 h, (b) 1 h, and (c) 15 h milled samples.

After one hour of ball milling, the particles are agglomerated due to the collision of the balls and the powder particles. This agglomeration provides a suitable condition for the solution of materials. Further milling leads to the formation of the final phases, which is accompanied by the separation of the particles. In the 15 h ball milled samples, narrow distributions of agglomerates are observed with particle size of about 10 μm.

3.2. Magnetic results

Figure 5 shows the real part of the AC susceptibility (χ') as a function of the temperature for $Co_2Cr_{1-x}Fe_xAl$ powder compounds after 0 h, 10 h, and 15 h of milling measured in an AC field of 10 Oe at the frequency of 333 Hz.

As expected, for all compounds, the susceptibility increases with the increasing milling time. It is clear that the increase of susceptibility in the ball milled powder is due to the formation of the $L2_1$-$Co_2Cr_{1-x}Fe_xAl$ Heusler phase. The paramagnetic–ferromagnetic transition temperature T_c of the $L2_1$-Co_2CrAl alloy is estimated to be about 340 K.[27] The maximum temperature we could measure is only 325 K. However the Curie temperature of the Co_2-based Heusler compounds is linearly dependent on the number of valence electrons.[6] In $Co_2Cr_{1-x}Fe_xAl$, the magnetic transition temperature increases with the increasing Fe content, as expected. Teresa *et al.* synthesized the $Co2Cr_{1-x}Fe_xAl$ series and measured the Curie temperatures of the samples. They reported that the magnetic transition temperature occurs at 840 K for $Co2Cr_{0.6}Fe_{0.4}Al$ and at higher than 850 K for Co2FeAl.[25] Figure 6 shows the variation of the susceptibility of the samples with Fe content x at room temperature. The susceptibility increases with the increasing Fe content, which is due to the increase of the magnetization of these compounds due to the Fe doping, as explained below.

Magnetization measurements on the 15 h ball milled samples were performed. Figure 7 shows the hysteresis loops of the samples at room temperature. The figure shows that M_s increases with the increasing Fe content. All of the loops are symmetric.

Figure 8 provides a comparison of M_s of the samples with the Slater Pauling curve and the Karthik samples.[13] As can be seen, for all of the samples, M_s is less than the estimated Slater Pauling value. In the previous work on bulk Co-based Heusler alloys, similar behaviour has been reported.[28] It is evident that there is no fundamental difference in magnetic behaviour between these nanostructured powder samples and the bulk compounds.

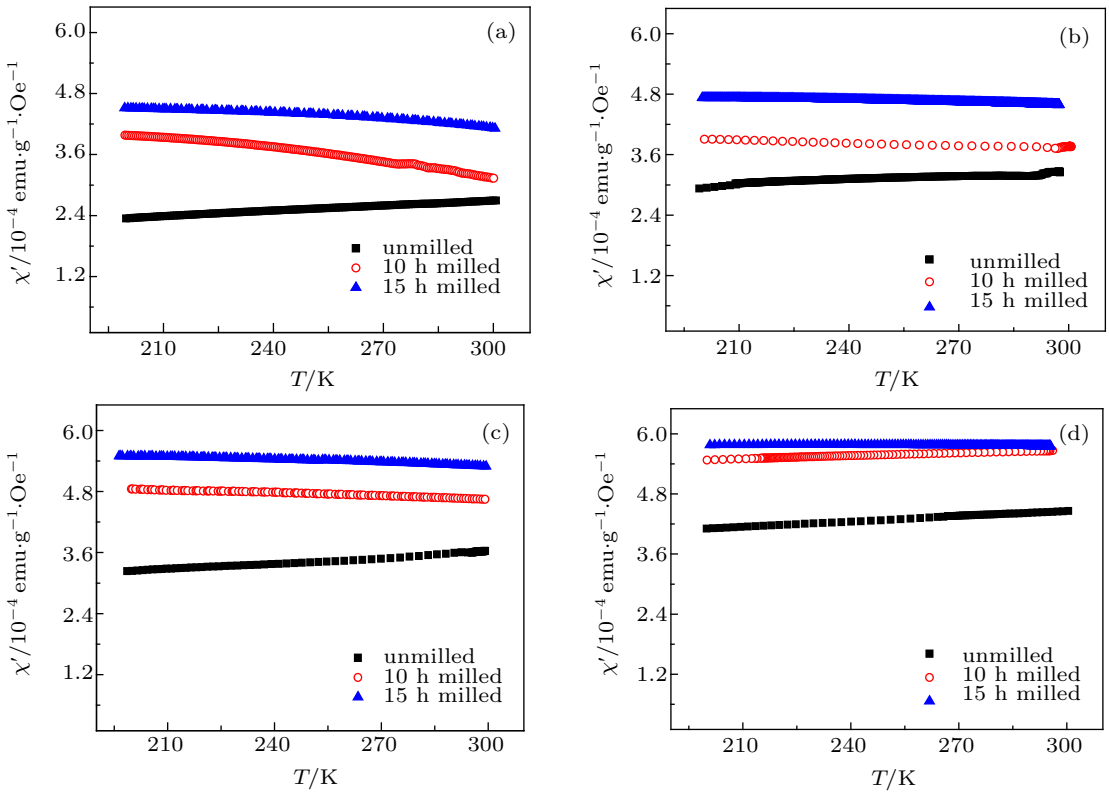


Fig. 5. (colour online) The real part of AC susceptibility (χ') fo $Co_2Cr_{1-x}Fe_xAl$ powder compounds after 0 h, 10 h, and 15 h of milling ((a) $x = 0$, (b) $x = 0.4$, (c) $x = 0.6$, (d) $x = 1$).

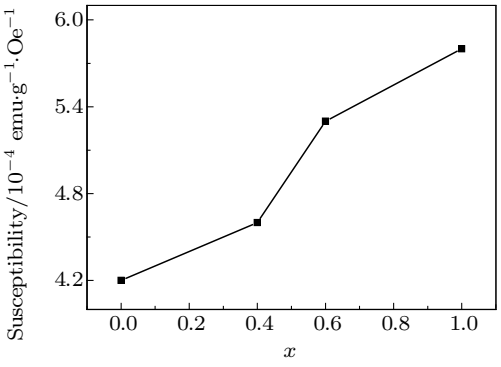


Fig. 6. The AC susceptibility of $Co_2Cr_{1-x}Fe_xAl$ samples at room temperature.

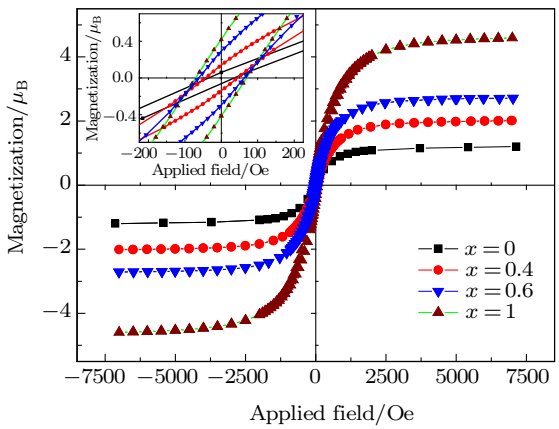


Fig. 7. (colour online) The magnetic hysteresis loops of $Co_2Cr_{1-x}Fe_xAl$ samples at room temperature. The inset shows the central part of the hysteresis loops on a larger scale.

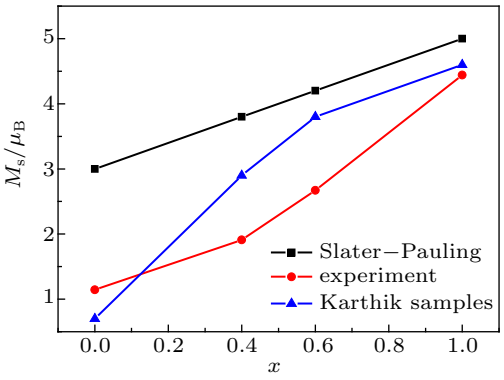


Fig. 8. (colour online) Comparison of M_s of the $Co2Cr_{1-x}Fe_xAl$ samples with the Slater Pauling curve and the Karthik samples.[13]

To explain the deviation from the Slater Pauling prediction, we review some of the previous reports on bulk and thin film samples. For example, Karthik *et al.*[13] have measured the saturation magnetization of the $Co2Cr_{1-x}Fe_xAl$ series. Their results are presented in Table 1. The values of M_s are lower than the Slater Pauling values. Inomata *et al.*[12] have reported a lower value of 1.1 μ_B for the magnetic moment of the $L2_1$-Co_2CrAl thin films. They have suggested that the atomic disorder in the crystalline $L2_1$–type ordered state depresses the ferromagnetic ordering in the alloy. Miura *et al.*[29] have predicted that the Cr atoms

occupy the Co sites in the $L2_1$ structure and antiferromagnetically couple with the Cr atoms. This can lead to a reduction of the magnetic moment for the samples with low doping levels. For the samples containing Fe, the measured magnetic moment is lower than the Slater Pauling prediction, but the difference decreases with the increasing Fe content.[30] In our case, the ball milling may induce some extra disorder and consequently decreases the magnetic moment. It is also well known that the magnetic moment of the ferromagnetic powder sample is smaller than that in the bulk due to the surface effects.[31] These effects can appear as (i) vacancies, (ii) breakings of chemical bounds, (iii) deviation of stoichiometric composition, (iv) termination of crystal structure, and (v) dislocation.[32] The other point is that the deviation from the Slater Pauling behaviour decreases with the increasing Fe content. The smaller value of M_s at the small Fe concentration has been attributed to a very low moment at the Cr sites.[28] For a better comparison of the coercivity H_c and the remanence M_r of the samples, the central part of the hysteresis loop is shown in the inset of Fig. 7 on a larger scale. The values of H_c and M_r are also provided in Table 1. It can be seen that these two parameters decrease with the decreasing Fe content. The H_c is heavily influenced by the magnetic anisotropy, including the magnetocrystalline and the strain induced anisotropy. Therefore, the decrease of H_c could be related to the decrease of the lattice strain and magnetocrystalline anisotropy with the increasing Cr content. As shown in Fig. 9, the relative reduction of M_r is more prominent than that of H_c. To explain this phenomenon, it should be noted that in addition to the decrease of lattice strain, the reduction of magnetic moment per unit cell can play an additional role in decreasing M_r.

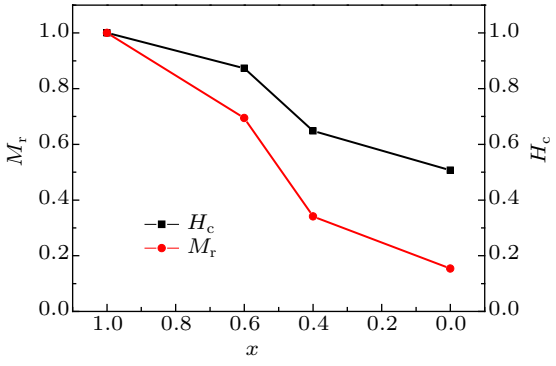


Fig. 9. (colour online) The relative reductions of M_r and H_c with the decreasing Fe content.

4. Conclusion

The mechanical alloying of Co, Cr, Fe, and Al powders for about 15 h leads to the formation of $L2_1$-$Co_2Cr_{1-x}Fe_xAl$ nanostructured Heusler alloy powders. The magnetic moment per unit formula increases with the increasing Fe content due to the higher magnetic moment of the Fe ions. The deviation of the magnetic moment per unit formula from the theoretical Slater Pauling value decreases with the increasing Fe content, which is attributed to a very low moment at the Cr sites. The H_c and M_r decrease with the decreasing Fe content. The decrease of H_c could be related to the reductions of lattice strain and magnetocrystalline anisotropy with the smaller Fe content.

Acknowledgement

The authors would like to thank Isfahan University of Technology for supporting this project.

References

[1] Coey J M D and Venkatesan M 2002 *J. Appl. Phys.* **91** 8345
[2] Picket W E and Singh D J 1997 *J. Magn. Magn. Mater.* **172** 237
[3] Akinaga H, Manago T and Shirai M 2000 *Jpn. J. Appl. Phys.* **39** L1118
[4] Li G N, Jin Y J and Lee J I 2010 *Chin. Phys.* B **19** 097102
[5] Felser C, Fecher G H and Balke B 2007 *Angew. Chem.* **46** 668
[6] Graf T, Felser C and Parkin S S P 2011 *Progress in Solid State Chemistry* **39** 1
[7] Chadov S, Qi X, Kübler J, Fecher G H, Felser C and Zhang S C 2010 *Nat. Mat.* **9** 541
[8] Engen P G van, Bushow K H J, Jongebreuer R and Erman M 1983 *Appl. Phys. Lett.* **42** 202
[9] Fu B, Long Y, Duan J F, Wang C L, Chang Y Q, Ye R C and Wu G H 2010 *Chin. Phys.* B **19** 097501
[10] Li Z, Jing C, Zhang H L, Cao S X and Zhang J C 2011 *Chin. Phys.* B **20** 047502
[11] Tian X H, Sui J H, Zhang X, Feng X and Cai W 2011 *Chin. Phys.* B **20** 047503
[12] Inomata K, Ikeda N, Tezuka N, Goto R, Sugimoto S, Wojcik M and Jedryka E 2008 *Sci. Technol. Adv. Mater.* **9** 14101
[13] Karthik S V, Rajanikanth A, Takahashi Y K, Ohkubo T and Hono K 2007 *Acta Materialia* **55** 3867
[14] Block T, Felser C, Jakob G, Ensling J, Muhling B, Gutlich P and Cava R J 2003 *J. Solid State Chem.* **176** 646
[15] Wurmehl S, Morais J, Carmo M do, Alves M, Teixeira S R, Fecher G H and Felser C 2006 *J. Alloy Compd.* **123** 159
[16] Ismayadi I, Mansor H, Khamirul A M, Rosidah A and Jumiah H 2011 *J. Supercond. Nov. Magn.* **25** 71

[17] Liu Z, Chen R J, Li D and Yan A R 2010 *Chin. Phys.* B **19** 067504
[18] Hatchard TD, Thorne J S, Farrell S P and Dunlap R A 2008 *J. Phys.*: *Condens. Matter* **20** 445205
[19] Vinesh A, Bhargava H, Lakshmi N and Venugopalan K 2009 *J. Appl. Phys.* **105** 07A309
[20] Bahrami H, Kameli P and Salamati H 2009 *J. Magn. Magn. Mater.* **321** 2533
[21] Mikami M, Matsumoto A and Kobayashi K 2008 *J. Alloy Compd.* **461** 423
[22] Hakimi M, Kameli P and Salamati H 2010 *J. Magn. Magn. Mater.* **322** 3443
[23] Hakimi M, Kameli P, Salamati H and Mazaheri Y 2012 *Powder Metall.* in press
[24] Lee M D, Lee J F, Chang C S and Dong T Y 1991 *Appl. Catalysis* **72** 267
[25] Teresa J M De, Serrate D, Cordoba R and Yusuf S M 2008 *J. Alloy Compd.* **450** 31
[26] Cullity B D and Stock S R 2002 *Elements of X-ray Diffraction* (3rd edn.) (Upper Saddle River: Prentice Hall)
[27] Carbonari A W, Saxena R N Jr, Pendl W, Mestnik Filho J, Attili R N, Olzon-Dionysio M and Souza S D de 1996 *J. Magn. Magn. Mater.* **163** 313
[28] Felser C, Elmers H J and Fecher G H 2005 *Lecture Notes in Physics* **676** 113
[29] Miura Y, Nagao K and Shirai M 2004 *Phys. Rev.* B **69** 144413
[30] Buchmeier M, Schneider C M, Werner J, Elefant D, Teresiak A, Behr G, Schumann J and Arushanov E 2007 *J. Magn. Magn. Mater.* **313** 157
[31] Kameli P, Salamati H and Aezami A 2006 *J. Appl. Phys.* **100** 053914
[32] Kameli P, Salamati H and Aezami A 2008 *J. Alloy Compd.* **450** 7